Phase Behavior, Crystallization Kinetics, and Morphology of Monotropic Liquid Crystalline Poly(ester−imide)s with a Decamethylene Spacer

Sang Ouk Kim, Chong Min Koo, In Jae Chung, and Hee-Tae Jung*

Department of Chemical Engineering, Korea Advanced Institute of Science and Technology, 373-1 Kusong-dong, Yusong-gu, Taejon 305-701, South Korea

Received July 27, 2001; Revised Manuscript Received October 7, 2001

ABSTRACT: The phase transition, crystallization kinetics, and morphology of monotropic liquid crystalline poly(ester−imide)s are investigated by synchrotron X-ray diffraction, differential scanning calorimetry (DSC), polarized light microscopy (PLM), and transmission electron microscopy (TEM). Synchrotron X-ray diffraction and DSC results show that the poly(ester−imide) with methyl side pendant group (10M) exhibits monotropic nematic and smectic A phases upon cooling from the isotropic melt, followed by a crystalline phase (crystal E structure). The results of isothermal crystallization kinetics show that the crystallization rate is faster in the smectic phase than in the nematic phase and the slowest in the isotropic phase. It is found that the crystallization in the nematic phase leads to lamellar decorated disclination structures upon TEM observation, indicating that the enhancement of nucleation dominates the acceleration of crystallization. Poly(ester−imide) without side pendant group (10H) forms only a crystalline phase upon cooling. However, the air-quenched sample shows a threadlike texture. TEM observation further reveals the trace of nematic disclination structures, confirming that the crystallization proceeds through nematic phase. In contrast, the sample, cooled with a slow cooling rate of 5 °C/min, exhibits the spherulite structure. The morphological variation of the poly(ester−imide) is discussed on the basis of competition between primary nucleation and crystal growth.

Introduction

The liquid crystalline phase of a monotropic liquid crystalline polymer is thermodynamically stable below its crystal melting temperature. The metastable liquid crystalline phase is temporarily observable only when crystallization is bypassed below the mesophase transition temperature with an adequate cooling rate.[1,2]

Because the monotropic liquid crystalline polymers crystallize from both monotropic liquid crystalline phase and supercooled isotropic phase, they provide good opportunities to study the effect of liquid crystalline ordering on the crystallization behaviors of polymeric materials.[1] The changes of crystal melting temperature,[3−5] Avrami exponent values for the crystallization,[6,7] and crystal structure[6b] in the presence of liquid crystalline ordering have been reported for various monotropic liquid crystalline polymers. MacKnight and co-workers[7] reported for a monotropic liquid crystalline polyurethane that the crystallizations from monotropic liquid crystalline phase and isotropic melt exhibit different Avrami exponent values, suggesting different crystallization mechanisms. Cebe and co-workers[3] demonstrated that the melting temperature of the crystal formed in the monotropic nematic phase is higher than that in isotropic melt for a monotropic liquid crystalline polycarbonate, which is interpreted by a model that nematic phase serves as nuclei for crystallization.[8] Cheng and co-workers conducted precise characterizations of the crystallization behavior for a series of monotropic liquid crystalline poly(ester−imide)s with smectic A phase.[6] They showed that the Avrami exponent value for crystallization in smectic phase is two, whereas the value in isotropic phase is three, and the wide-angle X-ray diffraction (WAXD) patterns of the crystal formed in monotropic smectic phase and isotropic phase were different for the poly(ester−imide)s with odd number of methylene spacers. In our previous articles, we synthesized liquid crystalline poly(ester−imide)s and characterized their monotropic phase transition behaviors with rheological methods.[5,9] The Avrami exponent value for crystallization was four in both isotropic and nematic phases, and the WAXD patterns of the crystallized samples are the same regardless of the precursor phase. The crystal formed from nematic phase showed the higher melting temperature than that from isotropic melt. From the previous crystallization studies on monotropic liquid crystalline polymers, the most significant conclusion is that the crystallization accelerates in the presence of liquid crystalline ordering.[1,3,5,6a,c,7−10] However, the mechanism for the acceleration of crystallization has been unknown.

In this article, we investigate the phase behaviors, crystallization kinetics, and crystal morphologies of monotropic liquid crystalline poly(ester−imide)s. Synchrotron X-ray diffraction, DSC, and PLM experiments determine the precise phase transition behaviors of the poly(ester−imide)s. The methyl side pendant group in the poly(ester−imide) strongly influences phase behavior, crystallization kinetics, and morphology. The morphological characterization of crystallized samples by TEM gives some insight into the origin of the enhancement of crystallization in liquid crystalline phase.

Experimental Section

The chemical structures of the monotropic liquid crystalline poly(ester−imide)s with a decamethylene flexible spacer are shown below. They are polymerized from *N*-(10-carboxydecanyl) trimellitic imide and hydroquinone or methylhydroquinone by melt transesterification reaction with MgO catalyst, as described in our previous publications.[5,9] We denote the poly(ester−imide) with methyl side pendant group as 10M and the polymer without methyl side pendant group as 10H.

* Corresponding author: e-mail heetae@kaist.ac.kr; Tel +82-42-869-3931; FAX +82-42-869-3910.

10.1021/ma011344s CCC: $20.00
Published on Web 11/22/2001

The inherent viscosities in *m*-cresol at 20 °C at a concentration of 0.5 g/dL are measured to be 0.71 for 10M and 0.25 for 10H.

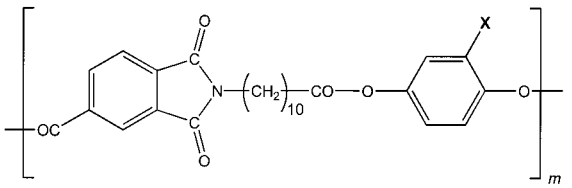

Structures of poly(ester-imide)s. **X**=H: 10H, **X** =CH_3: 10M.

The thermal transition behaviors and crystallization rates were performed on a Dupont 2010 thermal analyzer under N_2 flow at various scan rates. The crystallization rates were measured from isothermal crystallization experiments. Before each measurement, DSC was preequilibrated at the crystallization temperature. The samples, annealed above their melting temperature for several minutes to erase previous thermal history, were shifted to DSC, and the crystallization exotherm was recorded at each temperature.

Syncrotron X-ray scattering measurement was conducted with a wavelength of 1.54 Å at the 4C2 XRD beamline in Pohang Accelator Laboratory (PAL), consisting of 2 GeV LINAC accelerator, storage ring, Si (111) double crystal monochromator, ion chambers, and one-dimensional position-sensitive detector with 2048 pixels. A small amount of sample was sealed with imide films. Each sample was heated above the isotropic melt and then cooled with a cooling rate of 5 °C/min, which is the same as those of DSC cooling scans. The temperature was controlled with an accuracy of ±1 °C in the experimental temperature range.

The anisotropic optical textures were observed on a polarized optical microscopy (A Leitz, model Laborlux 12 Pols), equipped with a hot stage (Mettler FP82 HT). The thermal history of each sample was controlled as follows: The texture evolution of 10M was observed on the isothermal conditions. The sample was cooled from the isotropic melt to each annealing temperature with a rate of 5 °C/min. The thermal history of 10H was controlled with dynamic temperature protocol. Each sample was cooled from isotropic melt, varying the cooling rate (5 °C/min, 20 °C/min, and air quenching) to ambient temperature.

For the TEM observation, thin films were prepared by surface tension spreading on hot phosphoric acid above their melting temperatures.[11] After the spreading, the specimen was poured into cold water, which results in quenched thin films floating on the water surface. The films, showing the color of silver or weak gold, were carefully recovered on the carbon-supported Cu grids. The thermal history of the thin films was controlled in the same way as the samples for the polarized light microscopy observation. These samples were examined with a 120 kV PHILIPS CM-20 TEM. It has to be noted that all the thermal history control in this study started from the isotropic melt. Thus, all the morphology formations are spontaneous in each condition.

Results and Discussion

Phase Transition Behaviors. Figure 1 shows DSC cooling and subsequent heating scans of 10M and 10H samples. The scan rates were 5 and 10 °C/min for the cooling and heating, respectively. Upon the cooling scan of 10M, a major exothermic transition occurs at around 116 °C (5.4 kJ/mru), which is followed by two small transitions at 101 °C (1.7 kJ/mru) and 83 °C (2.9 kJ/mru). A glass transition appears at 39 °C. The high transition temperature at 116 °C was reported to be independent of cooling rates, indicating a low ordered mesophase transition.[5] The following heating scan exhibits the glass transition at 46 °C and only one endothermic transition at 147 °C (10.0 kJ/mru), which was characterized as crystal melting transition.[5] The

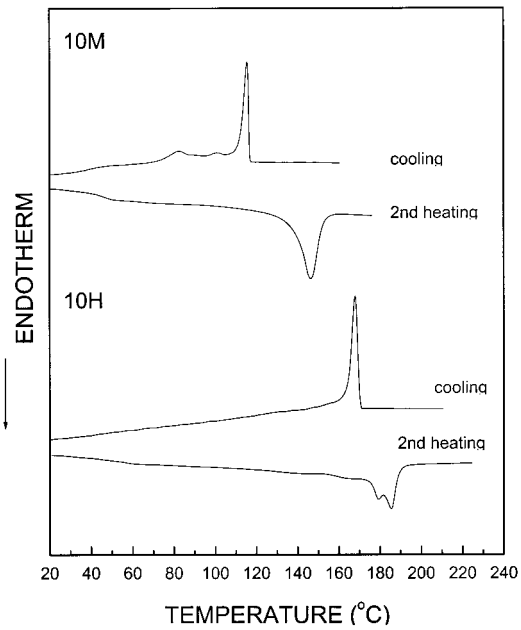

Figure 1. DSC thermograms of 10M and 10H upon cooling and following heating scan. The cooling rate and heating rates are 5 and 10 °C/min, respectively.

amount of heat for the melting transition agrees well with the sum of those of three exothermic transitions on the cooling scan. On the other hand, the cooling curve of 10H exhibits only one exothermic transition at 168 °C (19.2 kJ/mru), followed by a glass transition at 49 °C. Upon heating, the glass transition appears at 57 °C, and three sequential endothermic transitions appear around 163, 179, and 185 °C. The total amount of heat for the triple transitions corresponds to that of the exothermic transition on the cooling scan. The endothermic transitions were also verified as crystal melting ones in our previous work.[9]

To investigate the structural changes on the thermal transitions, synchrotron X-ray diffraction experiments were performed upon cooling with the same thermal history as in the DSC experiment (Figure 2). Each cooling scan starts from the isotropic phase of each polymer (above the crystal melting temperature). Figure 2a shows XRD patterns of 10M. The reflection peak at $2\theta \sim 5.9°$ corresponds to imide film scattering. Above 118 °C only an amorphous halo is observed. Around 116 °C, one can observe a suddern shift of the scattering maximum of the diffuse scattering halo (indicated by dark arrow), which is typical in the isotropic to nematic transition.[12] The shape of amorphous halo gets slightly sharper after the phase transition. The transition corresponds to the major exothermic transitions upon DSC cooling scan at the same cooling rate. This is also consistent with our previous rheological results for the 10M sample,[5] showing that the storage modulus and complex viscosity show the sudden decreasing behavior upon cooling at the same region, confirming the isotropic to nematic phase transition. Upon further cooling, a small angle peak at $2\theta \sim 3.63°$ (24.6 Å) starts to appear at around 108 °C. This represents that the smectic layers develop from the temperature. The maximum intensity at ~102 °C corresponds to the transition temperature of the small exotherm observed on the DSC cooling scan at the same rate. With a brief calculation, it is found that the *d* spacing of the small-angle peak (24.6 Å) corresponds to the full repeating unit having all-trans conformation of methylene spacers. Thus, the

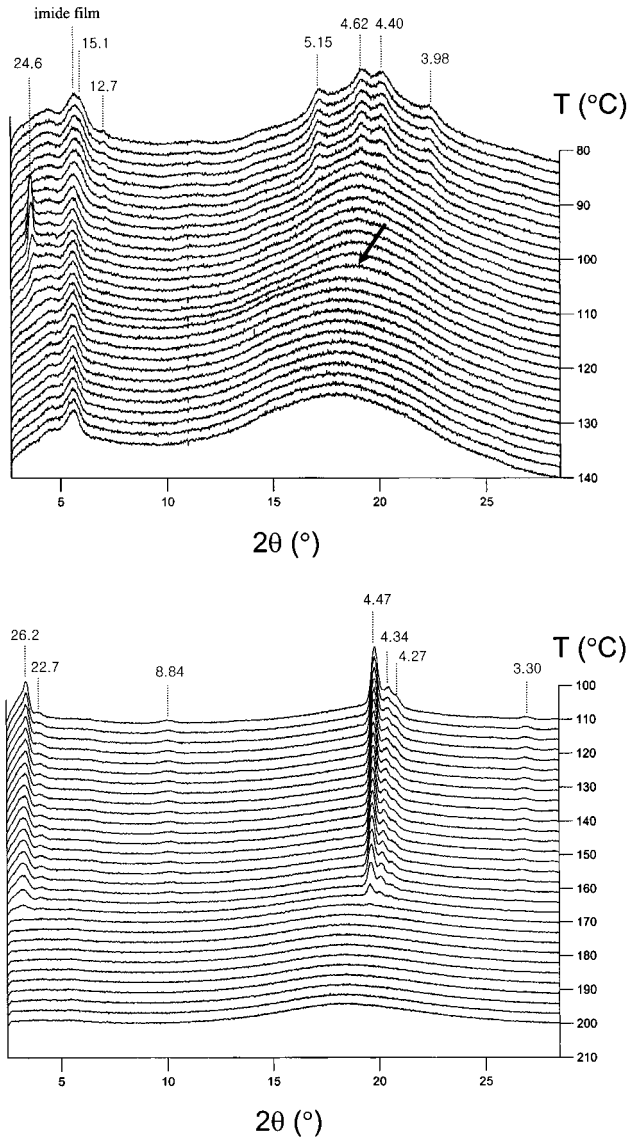

Figure 2. Synchrotron X-ray diffraction upon cooling from isotropic melt at the rate of 5 °C/min of (a, top) 10M and (b, bottom) 10H. The Kapton films were used to preserve the fixture in the molten state.

transition is assigned as a monotropic smectic A phase formation. Further cooling results in the crystallization with three-dimensional positional ordering. The crystal structure develops from ∼ 90 °C, and the wide-angle diffraction peaks clearly show the existence of an orthorhombic type of order, indicating that this phase is a smectic crystal E.[13] The phase transition temperatures of 10M characterized by DSC and synchrotron X-ray diffraction experiments upon cooling at 5 °C/min are summarized as follows:

isotropic (116 °C) nematic (101 °C)
smectic A (83 °C) crystal E

Because the nematic and smectic A phase transition temperatures are lower than the crystalline melting temperature, the nematic and smectic A phases are referred to as monotropic liquid crystalline phases. To the best of our knowledge, the present result is the first example that two kinds of monotropic liquid crystalline phases (monotropic nematic and smectic phases) are observed for a liquid crystalline polymer. The monotropic smectic phase formation was not detected in our previous rheological characterization.[5] It has been hard to discern the smectic phase transition, because both the smectic phase formation and crystallization yield the jump up of the rheological parameters.

The reason for the formation of the monotropic liquid crystalline phase can be understood on the basis of the molecular structure. Whether a liquid crystalline polymer is monotropic or enantiotropic depends on the relative stability of liquid crystalline phase and crystal phase. It is well-known that the length of aliphatic spacer unit and the mesogenic character of rigid unit affect the stability of mesophase in the semiflexible liquid crystalline polymers. The thermodynamic contribution of each unit can be separated, which results in the well-known odd−even effect of methylene spacer length.[6b,14] The molecular chain of 10M has a relatively randomized structure due to the asymmetric chemical structure of *N*-(10-carboxydecalyl) trimellitic imide unit. Thus, the mesogenic character of rigid units should be poor with the randomized molecular structure. Moreover, the long aliphatic spacer length containing decamethylene unit acts a crucial role for the phase behavior. It was reported that the poly(ester−imide) constituted of the same rigid unit with 10M but containing butylenes or hexamethylene spacer formed enantiotropic nematic phase.[15] Although the methylene unit of semiflexible liquid crystalline polymer participates in the ordering of a mesophase, the thermodynamic contributions are known to be lower than those of mesogenic units.[14] As a result, the longer the methylene spacer length, the lower the mesophase to isotropic phase transition temperature. In contrast, the lowering of crystallization temperature slows down at some length of methylene spacer. It is based on the principle that the stability of a crystal phase depends on the regularity of molecular structure. The methylene spacer with a long length dominates the regularity of the molecular structure.

Compared to the monotropic liquid crystalline transition behavior of 10M, 10H does not show monotropic liquid crystalline transition upon cooling from the isotropic melt, based on the DSC and XRD results. As shown in Figure 2b, the crystallization proceeds directly from isotropic melt. The layer spacing of 26.2 Å (2θ = 3.37°) corresponds to the full length of the repeating unit of polymer chain with all-trans conformation of methylene spacers. Although these DSC and XRD results do not show any evidences of monotropic liquid crystalline transition, we are not able to exclude a possibility that the crystallization of 10H proceeds through monotropic nematic phase upon cooling, just because of very fast crystallization process on the sample.[9] In other words, development of these phases may overlap during the crystallization process. The detailed discussion will be presented in the morphology evolution section.

Crystallization Rate and Morphology of 10M. Figure 3 shows the crystallization rate of 10M at various temperatures. The time to reach half-conversion of crystallization is measured at each temperature, and the inversion of it is used as an indication for the crystallization rate. It should be noted that the phase transition behavior described in the previous section is based on the experiments upon cooling at 5 °C/min. Thus, the transition temperatures may include the kinetic effect of the measuring condition. To identify the phase transition temperatures, the transition temper-

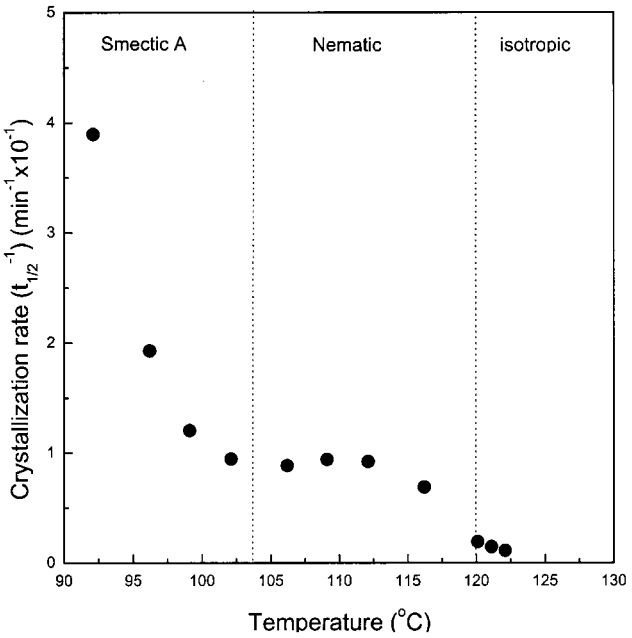

Figure 3. Crystallization rates at various temperatures for 10M. The precursor phase for crystallization is indicated.

atures observed in the DSC cooling at various scan rates were extrapolated to the value at the zero cooling rate. The isotropic to nematic transition and the nematic to smectic transition temperatures without kinetic effect are found to be 119.7 and 103.7 °C, respectively. Those temperatures were used to determine the temperature range of the precursor phase for crystallization.

In general, the ideal crystallization rate of a polymer shows the inverted "U" shape, which is the fastest at some temperatures between the glass transition and melting temperature. Cheng and co-workers[6c] have reported for a series of monotropic liquid crystalline polymers that the crystallization rates in monotropic smectic and supercooled isotropic phases are independent, which result in discontinuity at the smectic to isotropic phase transition temperature. In Figure 3, there is a maximum rate around 110 °C for nematic phase. The crystallization rate is too slow below 90 °C and too fast above 123 °C to be detected with DSC so that the measuring temperature range is restricted for the monotropic smectic and supercooled isotropic phase.

Despite the limitation of the experimental temperature range, the crystallization rate shows clear transitions with the changes of precursor phase. The crystallization rate is the fastest in the smectic phase and decreases as a function of the degree of ordering of the precursor phase (smectic A > nematic > isotropic). The earlier publications regarding various monotropic liquid crystalline polymers show that the crystallization rates in liquid crystalline phases (nematic or smectic phase) are higher than that in isotropic phase.[1,3,5,6a,c,7−10]

To further understand the crystallization kinetics, the morphology formations on the crystallization at various temperatures are investigated. Figure 4a shows the polarized light micrograph of 10M on the isothermal annealing at 125 °C, which is in the temperature range of the supercooled isotropic melt. The sample was completely melted above 160 °C and cooled at 5 °C/min to the annealing temperature. Supramolecular crystal structure grows from the isotropic melt, following typical nucleation and growth mechanism. A transmission electron micrograph of the supramolecular structure is

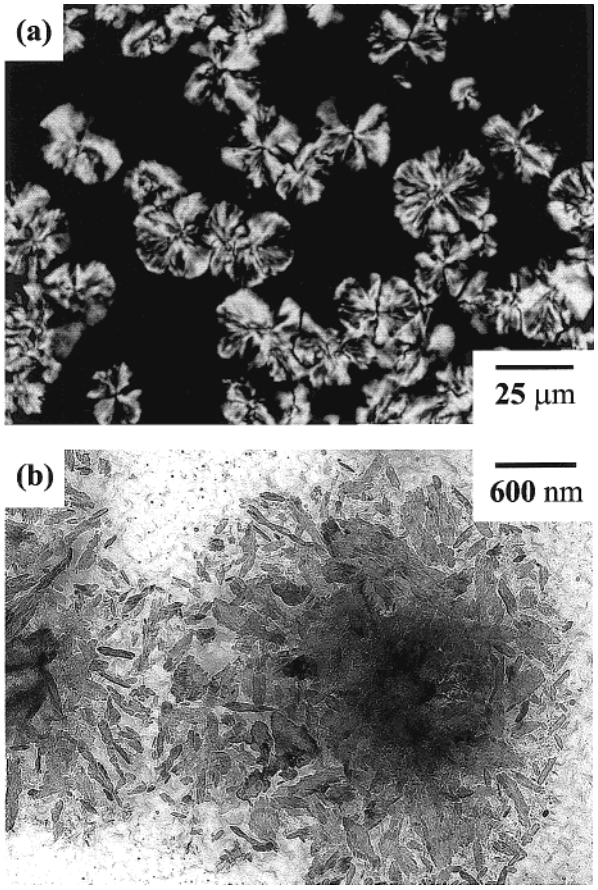

Figure 4. (a) Polarized light micrograph upon isothermal annealing at 125 °C and (b) transmission electron micrograph of 10M, isothermally annealed at the same temperature. The samples were cooled from an isotropic melt to the annealing temperature at the rate of 5 °C/min.

shown in Figure 4b. A somewhat randomized arrangement of lamellae appears to be a hedrite type crystal.[16]

Figure 5a shows the polarized light micrograph of the sample annealed at 118 °C, which is in the range of the monotropic nematic phase. The sample was cooled from isotropic melt (160 °C) at 5 °C/min to the annealing temperature. The annealing time was long enough for the completion of crystallization. The morphology keeps a threadlike texture of liquid crystalline phase upon crystallization. The distinct morphological change with the liquid crystalline ordering has been reported for various monotropic liquid crystalline polymers.[5,6a,7] It has been reported that crystallization proceeds through usual nucleation and growth mechanism in the isotropic phase, but the texture of liquid crystalline phase persists until the completion of crystallization in the nematic phase. To confirm the structure and origin of the crystallization, the TEM experiment is conducted for a sample with the same thermal history. The TEM image shows disclination structures in the field of oriented lamellae as shown in Figure 5b, which is termed the lamellar decoration morphology. The lamellae decorate the nematic director field without observable alternation of the chain axis from the precursor nematic to the semicrystalline state.[17] The image also shows disclinations which introduce distortion into the director filed. Considering the disclinations are characteristic of preexisted nematic liquid crystal, the structure is clearly identified as nematic phase. The lamellar decoration method was occupied to observe the molecular director distribution of nematic phase directly

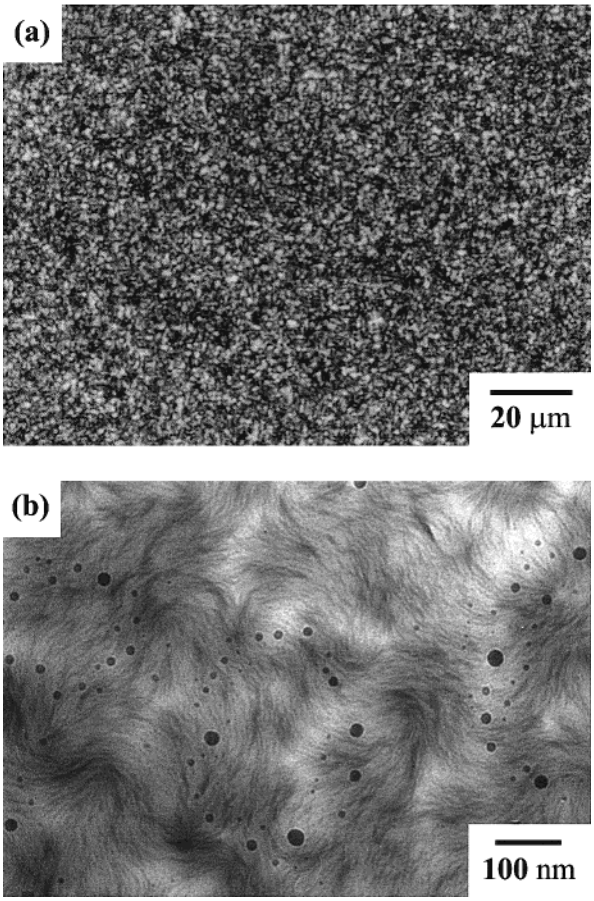

Figure 5. (a) Polarized light micrograph and (b) transmission electron micrograph of 10M, which is isothermally annealed at 118 °C. The samples were cooled from an isotropic melt to the annealing temperature at 5 °C/min.

through the enhanced contrast mechanism of lamellaes. The orientation of the polymer chain is known to be perpendicular to the long dimension of lamella from the selected area electron diffraction result.[17b]

As described previously, one of the most prominent characteristics in the crystallization of monotropic liquid crystalline polymers is the acceleration of crystallization in liquid crystalline phase.[1,3,5,6a,c,7−10] Generally, the crystal morphology of a polymer is determined by the competition between the nucleation and growth. With a high density of primary nuclei, the crystallization proceeds through the growth of lamellae, which reflects the molecular arrangement of melt state. On the contrary, the massive chain rearrangement would occur during the growth of a supramolecular structure with a low density of nucleus. The lamellar decorated morphology formation in nematic phase implies the high density of nucleation upon crystallization, because it develops when nucleation is rapid and growth slow. Except the spontaneous formation of the precursor ordered state, the crystallization from nematic phase resembles that of oriented polymer chains.[18] One may speculate that the primary nucleation is easier in nematic phase due to the extended chain conformation and low surface energy at crystal. As a result, the enhancement of crystallization rate in the nematic phase must be dominated by the acceleration of the primary nucleation. The same principle may be applicable to most of liquid crystalline polymers, which persists the morphology of liquid crystalline phase on crystallization.

The morphology by the crystallization in the smectic phase is similar to that in the nematic phase, showing threadlike texture on polarized light microscopy (not shown here). Thus, the fast nucleation dominates the crystallization in smectic A phase as in the nematic phase. Further acceleration of crystallization in the smectic phase seems to be attributed to the formation of layer structure. With the ultimate crystal structure of crystal E type, the smectic layer structure may enhance crystallization. The energy barrier for nucleation may be the lowest in smectic phase due to the two-dimensional molecular ordering.

Morphology Evolution of 10H. Figure 6a,b shows a polarized light micrograph and TEM of 10H, air-quenched from isotropic melt. Despite the direct crystallization from isotropic melt (see Figures 1 and 2b), the morphology shows a threadlike texture, revealing the existence of a nematic phase. Similar lamellar decorated morphology is observed in this specimen, which is further evidence of crystallization process through a nematic phase. In our previous article,[9] DSC cooling scans with various cooling rates from 10 to 160 °C/min exhibited only a crystallization exotherm (the exotherm at 168 °C upon cooling scan of 10H in Figure 1). However, the crystallization exotherm persists its peak temperature and the amount of heat release upon the large change of cooling rates, which is typical in the low ordered liquid crystalline phase transition following the near-equilibrium process.

The only difference between molecular structures of 10H and 10M is the absence of a methyl side pendant group on the hydroquinone unit. The existence of methyl side pendant group gives irregularity on the molecular structure, because it provides the head-to-tail effect to the hydroquinone unit. The crystallization is greatly hampered with the more randomized molecular structure of 10M. On the contrary, the mesogenic property of rigid unit is not so severely affected, because the aspect ratio of the rigid-rod mesogenic unit decreases little with the methyl side pendant group.

The sample cooled at 20 °C/min shows a complex morphology, as shown in Figure 6c,d. Larger domains are seen, but their shape is randomized. It does not show any optical sign in quarter wave retardation plate test, which means that there is no macroscopic ordering of molecular chain in the crystal domains. Figure 6e,f shows the morphologies of 10H, cooled from isotropic melt at a cooling rate of 5 °C/min. The fully grown supramolecular structure of crystal is shown. The formation of structure follows the usual nucleation and growth mechanism. Upon the structure growing, a positive optical sign is clearly observed under a quarter-wave retardation plate.

The distinct morphological variation of 10H should be attributed to the change of nuclei density. The broad temperature range of the isotropic to nematic phase transition, which is intrinsic property of polydisperse liquid crystalline polymers,[19] might have acted a critical role. The fast cooling rate of air quenching may reduce the effect of broad transition range so that the whole sample crystallizes through nematic phase almost simultaneously. In that case, the nucleation should have occurred evenly on the sample, and the arrangement of lamellae shows the trace of the precursor nematic phase. Conversely, upon a slow cooling process, the high molecular weight portion should crystallize ahead through nematic phase and act as nuclei for the follow-

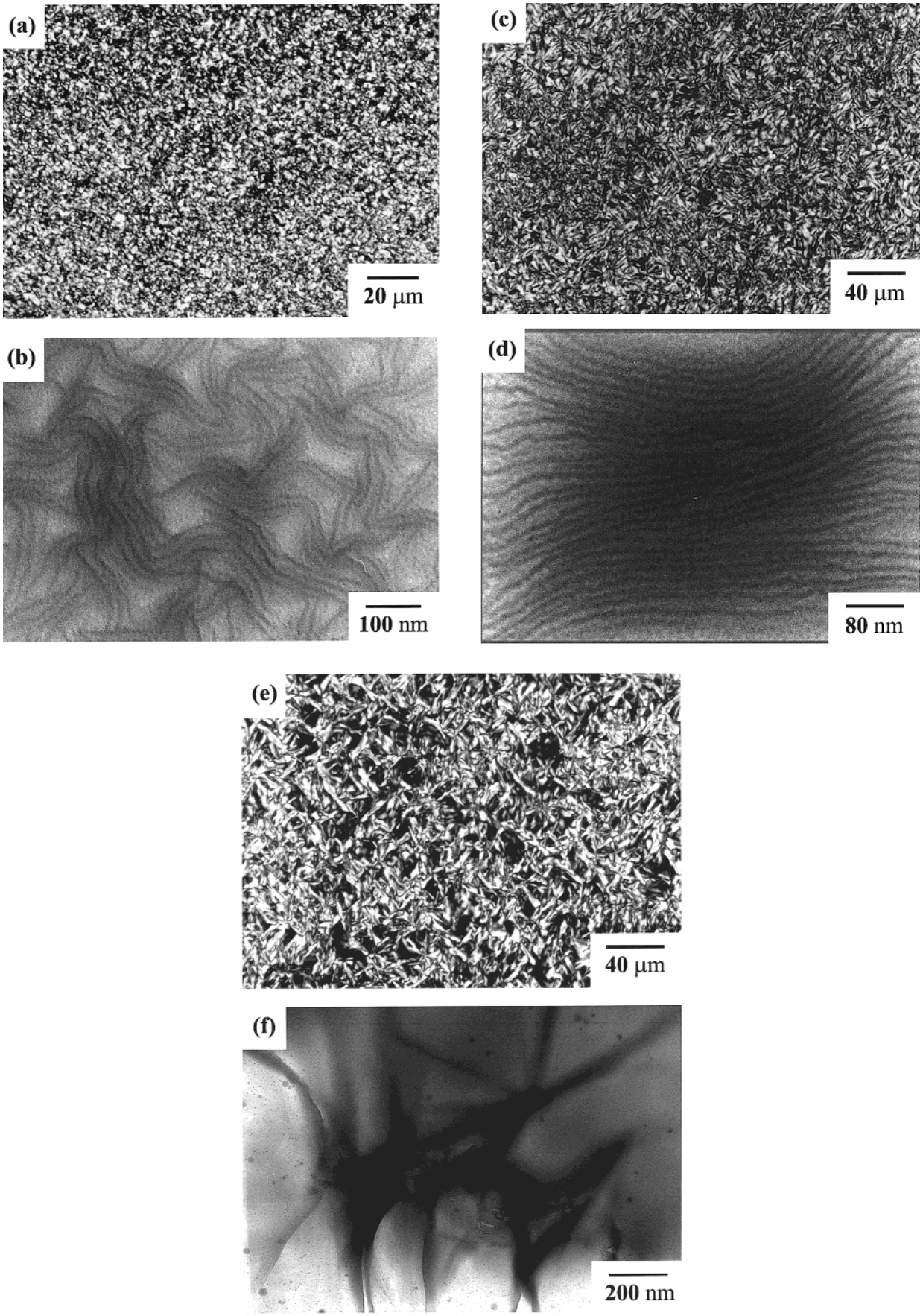

Figure 6. Polarized light micrographs and transmission electron micrographs of 10H cooled from isotropic melt with various cooling rates: (a) polarized light micrograph of air-quenched sample, (b) transmission electron micrograph of air-quenched sample, (c) polarized light micrograph of the sample cooled at 20 °C/min, (d) transmission electron micrograph of the sample cooled at 20 °C/min, (e) polarized light micrograph of the sample cooled at 5 °C/min, (f) transmission electron micrograph of the sample cooled at 5 °C/min.

ing crystallization. The secondary or tertiary nucleation rates may increase through nematic phase with reduced energy difference from crystal. Because of the high mobility along chain direction, the short-range diffusion of polymer backbone may get faster with liquid crystalline ordering.

Conclusion

The crystallization behaviors and morphological characteristics of monotropic liquid crystalline poly(ester−imide)s were investigated. Although the overall crystallization rate of 10H (without methyl side pendant group) is faster than that of 10M (with methyl side pendant group), both polymers have a common feature that the crystallization from liquid crystalline phase is much faster than that from isotropic phase. Synchrotron X-ray and DSC experiments reveal the sequential phase transition through isotropic, nematic, smectic A, and crystal E phase upon cooling process of 10M. In contrast, the existence of liquid crystalline phase of 10H was not detected, due to their very fast crystallization process.

The crystallization kinetics experiments show that the crystallization rate transits with the variation of the precursor phase for crystallization. The crystallization rate decreases sequentially as follows: monotropic smectic A phase−monotropic nematic phase−supercooled isotropic melt. The isothermal annealing of 10M in the supercooled isotropic temperature range leads to a spherulite structure. In contrast, the crystallization in nematic phase results in the lamellar decorated morphology, which verifies that the acceleration of crystallization is dominated by the enhancement of primary nucleation. The further acceleration of crystallization in smectic phase seems to be related with the layer structure formation. The morphology of 10H, air-quenched from the isotropic phase, shows the trace of nematic structure, which is the direct evidence of the monotropic phase transition behavior of this polymer. The morphologies are strongly influenced by the cooling rate. The fully grown spherulite structure is observed for the sample cooled at the slowest rate of 5 °C/min. The variation of morphology is discussed on the basis of changes of nucleation density. The growth rate as well as the nucleation rate seems to get faster in the presence of nematic ordering.

Acknowledgment. This work was supported in part by the Korea Science & Engineering Foundation (KOSEF) through Engineering Research Center (ERC) and in part by the Brain Korea 21 program. Experiments at Pohang Light Source (PSL) were supported in part by MOST and POSCO.

References and Notes

(1) (a) Keller, A.; Cheng, S. Z. D. *Polymer* **1998**, *39*, 4461−4487. (b) Cheng, S. Z. D.; Keller, A. *Annu. Rev. Mater. Sci.* **1998**, *28*, 533−562.
(2) Percec, V.; Keller, A. *Macromolecules* **1990**, *23*, 4347−4350.
(3) Cheng, Y. Y.; Cebe, P.; Schreuder-Gibson, H.; Bluhm, A.; Yeomans, W. *Macromolecules* **1994**, *27*, 5440−5448.
(4) Yandrasits, M. A.; Chen, J.; Arnold, F. E., Jr.; Cheng, S. Z. D.; Percec, V. *Polym. Adv. Technol.* **1994**, *5*, 775−784.
(5) Kim, S. O.; Chung, I. J. *Macromolecules* **2000**, *33*, 7549−7556.
(6) (a) Pardey, R.; Zhang, A.; Gabori, P. A.; Harris, F. W.; Cheng, S. Z. D.; Adduci, J.; Facinelli, J. V.; Lenz, F. W. *Macromolecules* **1992**, *25*, 5060−5068. (b) Pardey, R.; Wu, S. S.; Chen, J.; Harris, F. W.; Cheng, S. Z. D.; Keller, A.; Aducci, J.; Facinelli, J. V.; Lenz, R. W. *Macromolecules* **1993**, *26*, 3687−3697. (c) Pardey, R.; Wu, S. S.; Chen, J.; Harris, F. W.; Cheng, S. Z. D.; Keller, A.; Adduci, J.; Facinelli, J. V.; Lenz, F. W. *Macromolecules* **1994**, *27*, 5794−5802.
(7) Smyth, G.; Valles, E. M.; Pollack, S. K.; Grebowicz, J.; Stenhouse, P. J.; Hsu, S. L.; MacKnight, W. J. *Macromolecules* **1990**, *23*, 3389−3398.
(8) Cheng, Y.; Cebe, P.; Capel, M.; Schreuder-Gibson, H.; Bluhm, A. *J. Polym. Sci., Polym. Phys.* **1995**, *33*, 2331−2341.
(9) Kim, S. O.; Jeon, B. H.; Chung, I. J. *Polymer* **2001**, *42*, 3249−3257.
(10) Heberer, D.; Keller, A.; Percec, V. *J. Polym. Sci., Polym. Phys.* **1995**, *33*, 1877−1894.
(11) Jung, H.-T.; Hudson, S. D.; Lenz, R. *Macromolecules* **1998**, *31*, 637−643.
(12) Ungar, G.; Feijoo, J. L.; Keller, A.; Yourd, R.; Percec, V. *Macromolecules* **1990**, *23*, 3411−3416.
(13) Kricheldorf, H. R.; Probst, N.; Schwarz, G.; Wutz, C. *Macromolecules* **1996**, *29*, 4234−4240.
(14) Blumstein, A.; Thomas, O. *Macromolecules* **1982**, *15*, 1264−1267.
(15) Kim, S. O.; Chung, I. J. *Polymer* **2000**, *41*, 4709−4717.
(16) Geil, P. H. *Polymer Single Crystals*; Robert E. Krieger Publishing Co.: New York, 1973.
(17) (a) Wood, B. A.; Thomas, E. L. *Nature* **1986**, *324*, 655−657. (b) Thomas, E. L.; Wood, B. A. *Faraday Discuss. Chem. Soc.* **1985**, *79*, 229−239. (c) Hudson, S. D.; Thomas, E. L. *Phys. Rev. Lett.* **1989**, *24*, 1993−1996. (d) Hudson, S. D.; Thomas, E. L. *Chemstracts Macromol. Chem.* **1991**, *2*, 73−93.
(18) (a) Keller, A.; Machin, M. J. *J. Macromol. Sci., Phys.* **1967**, *B1*, 41−91. (b) Zhao, Y.; Keroack, D.; Prud'homme, R. *Macromolecules* **1999**, *32*, 1218−1225.
(19) (a) Nakai, A.; Wang, W.; Hashimoto, T.; Blumstein, A.; Maeda, Y. *Macromolecules* **1994**, *27*, 6963−6972. (b) Nakai, A.; Wang, W.; Hashimoto, T.; Blumstein, A. *Macromolecules* **1996**, *29*, 5288−5296.

MA011344S